Electronic Supplementary Material (ESI) for RSC Advances.

Synthesis and Extensive Characterisation of Phosphorus Doped Graphite

Peter D. Matthews,[a] Timothy C. King,[a] Hugh Glass,[a,b] Pieter C. M. M. Magusin,[a] Gary J. Tustin,[c] Philip A. C. Brown,[b] Jonathan A. Cormack,[a] Raúl García-Rodríguez,[a] Michal Leskes,[a] Siân E. Dutton,[b] Paul D. Barker,[a] F. Malte Grosche,[b] Ali Alavi,[a,d] Clare P. Grey,[a] Dominic S. Wright[a,*]

[a] Department of Chemistry, University of Cambridge, Lensfield Road, Cambridge, CB2 1EW (U.K.). E-mail: dsw1000@cam.ac.uk; Tel: +44 (0)1223 763122
[b] Cavendish Laboratory, University of Cambridge, JJ Thompson Ave., Cambridge, CB3 0HE (U.K.)
[c] Schlumberger Gould Research Centre, High Cross, Madingley Road, Cambridge, CB3 0EL (U.K.)
[d] Max Plank Institute for Solid State Research, Heisenbergstr 1, Stuttgart 70569 (Germany)

Contents

1. General Information

Common inert atmosphere techniques were followed for all syntheses using oven-dried glassware coupled to a standard Schlenk line operating under N_2. Solvents were freshly distilled over appropriate drying agents and stored under nitrogen, unless otherwise stated. All chemicals were purchased from Sigma-Aldrich.

2. Experimental Procedures

1,2-diphosphinobenzene
Synthesis adapted from Kyba *et al.*[1]
A solution of 1,2-dichlorobenzene (58.4 ml, 0.52 mol) and trimethyl phosphite (121.6 ml, 1.03 mol) underwent UV photolysis for 2 weeks. The solution was concentrated by vacuum distillation (40°C and 0.5 mmHg) and the residue left to crystallize at -20°C for 48h. Crystalline 1,2-bis(dimethylphosphite)benzene (5.80 g, 22 mmol) was collected at 5% yield. A slurry of $LiAlH_4$ (4.56 g, 120 mmol) in THF (100 ml) was cooled to -78°C and trimethylsilyl chloride (13 g, 120 mmol) added. The mixture was stirred at room temperature for 3h before 1,2-bis(dimethylphosphite)benzene was added slowly at -30°C and the reaction stirred at room temperature for 3 days. Water (100 ml) was added dropwise followed by 1M NaOH (100 ml) and then the two layers were separated. The aqueous layer was extracted with diethyl ether (2 x 100 ml) and the combined organic layers dried with $MgSO_4$ and then concentrated *in vacuo*. The residue was distilled at 50°C, 0.5 mmHg to give 1,2-diphosphinobenzene (1.20 g, 8.45 mmol) at 38 % yield.
^{31}P NMR: ($CDCl_3$) = -124.5 (s) (lit. -125.1)[1,2]

P-DG
In a typical synthesis, 0.15 ml of 1,2-diphosphinobenzene was loaded into an oven-dried quartz tube of dimensions 1.0 cm internal-diameter, 12.0 cm length (under N_2) and then evacuated to 10^{-3} Torr and flame-sealed. Carbonisation then took place in a Lenton LHB 12/600 two zone furnace, fitted with a ceramic weking tube and a Eurotherm 316 temperature controller. The temperature was ramped rapidly up to 800°C and held there for 1h before cooling to room temperature at a rate of 5°C/min. The quartz tube was opened in air and the P-DG extracted, washed in acetone and then oven-dried. To remove residual silica (left over from the reaction vessel) samples were matured overnight in aqueous HF (10 wt.%, 5 ml), washed with distilled-water (4 x 20 ml), acetone (4 x 20 ml) and finally oven-dried before any characterisation.

3. SEM

SEM were taken using a JEOL 5800 LV SEM with an acceleration voltage of 10kV. Figure S1 shows images of P-DG flakes.

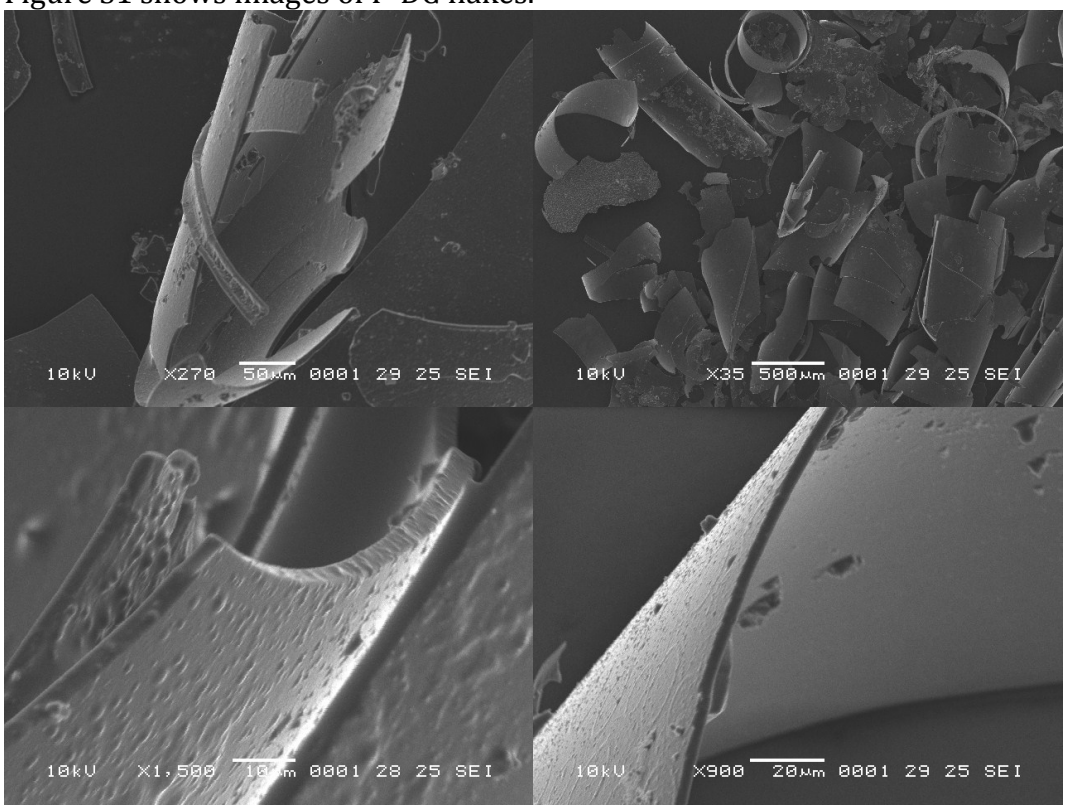

Figure S1. SEM images of P-DG.

4. XPS

X-ray Photoelectron Spectroscopy (XPS) was performed using a Thermo-Fisher K-Alpha XPS system with an EX06 Ion Source for depth profiling (Ar ion beam on the medium setting for 10 seconds at a time). CasaXPS software was used to process the data.

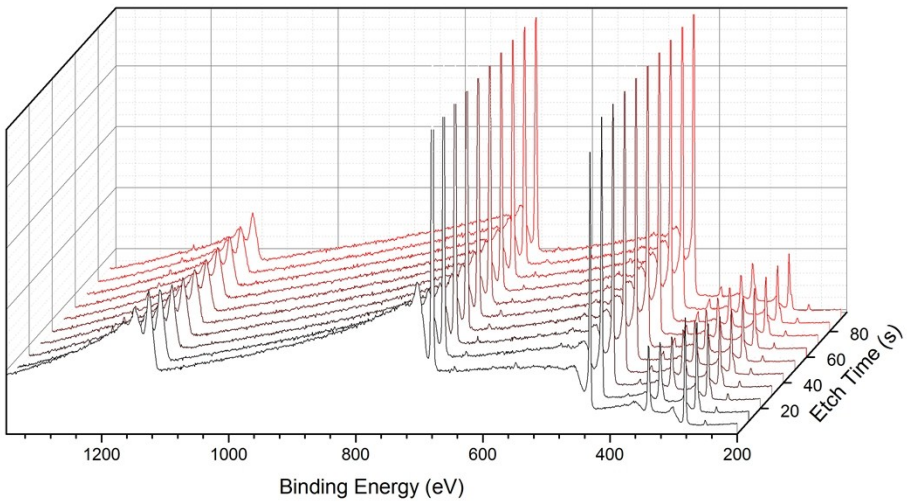

Figure S2. XPS depth plot of P-DG shows consistency throughout the sample.

a)

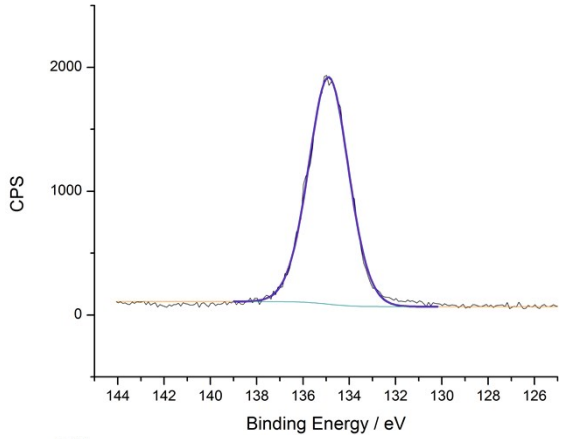

b)

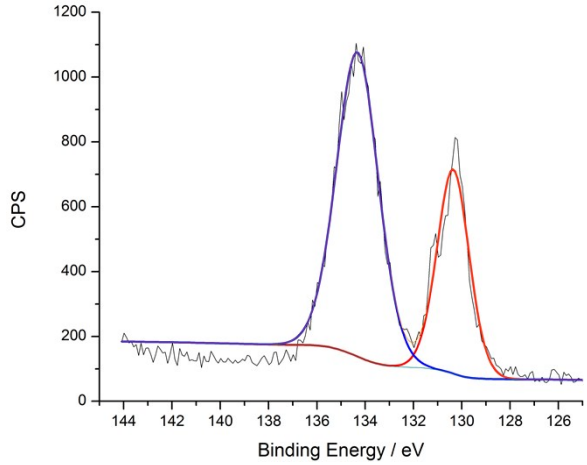

Figure S3. High resolution P 2P scans of the surface of a) unwashed surface of P-DG showing only a P=O environment and b) washed surface of P-DG showing the appearance of an elemental P_4 environment. Black is counts s^{-1}, teal is a Shirley baseline, blue is P=O, red is P_4 and orange the curve fitting.

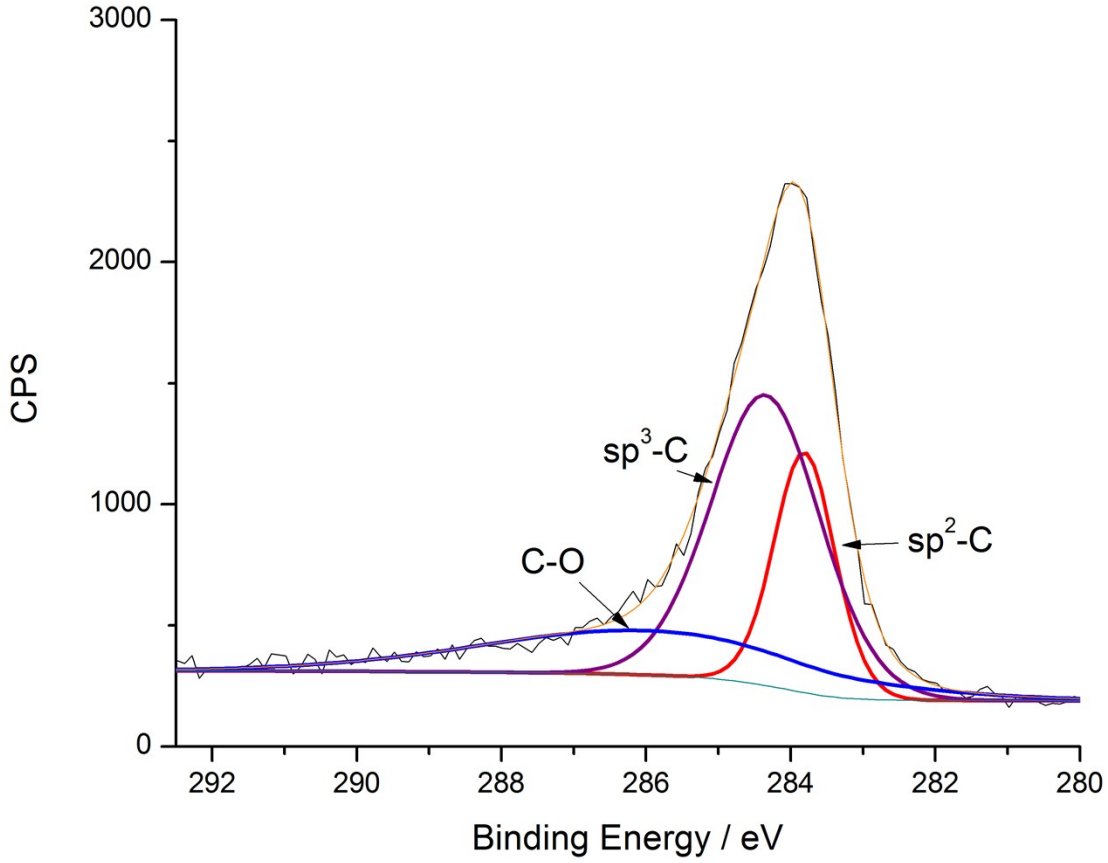

Figure S4. High resolution C 1s XPS scan. This, combined with figure 2c demonstrate some of the variability of the P-DG. Here only sp2 C (red), sp3 C (purple) and C-O (green) environments can be seen – there are no C-P bonds.

Part of the oxygen seen in the XPS analysis can be accounted for by the presence of adventitious oxygen and not just oxidation of the material. This was confirmed by a previous study.[3]

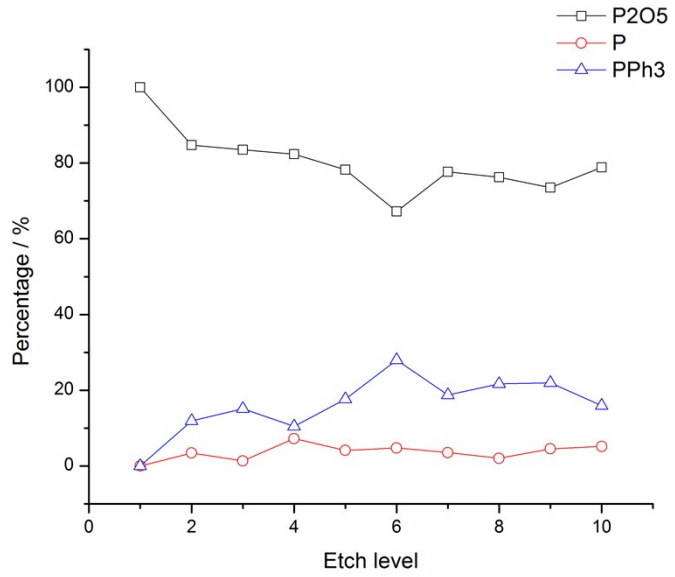

Figure S5. Depth profile of the different P environments as determined by XPS analysis.

5. MALDI-TOF

Matrix Assisted Laser Desorption/Ionisation-Time of Flight mass spectrometry was carried out using an Applied Biosystems Proteomics Analyser 4700. The P-DG presents peaks corresponding to the C_n and also to $^{31}P_n$. The P_n series continues to a higher m/z than the C_n series, producing clusters of greater than 20 atoms. This would correspond to the presence of phosphorous outside of the carbon lattice. The lack of oxidation may point to the generation of inclusions removed from the atmosphere. Strong phosphorus cluster signals appear intermittently during accumulations, with 155 m/z being particularly characteristic. This lends credence to the formation of small clusters or grains embedded in the carbon structure. Under positive MS-MS mode a small number of peaks corresponding to C_nP have been identified and broken down with the aid of CID gas to form other C_nP and C_n peaks. Unfortunately this alone is not enough to say whether the phosphorus is a covalently bound component of the hexagonal lattice or whether it is merely associated with the parent ion and the various daughter fragments that can be generated. However when these data are combined with the fact that the samples requires a significantly higher laser intensity than graphite to generate the C_n and C_nP signals it would suggest that some of the phosphorus has indeed been incorporated and changed the overall properties of the graphite.

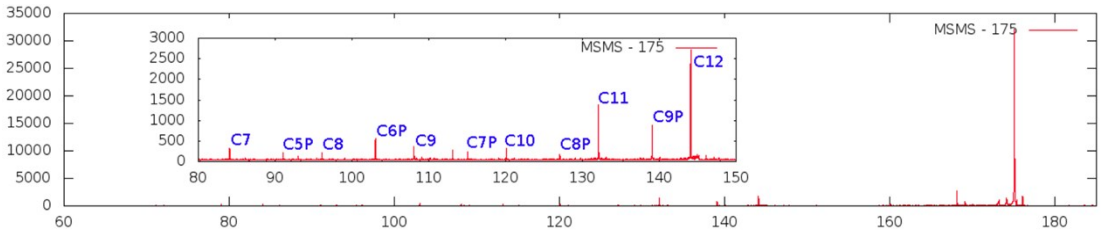

Figure S6. MS-MS of a parent ion of m/z = 175 with assignments of daughter ions.

6. Solid State NMR

Three different P-DG batches #1, #2 and #3 were investigated by use of fast magic-angle spinning (MAS) NMR. ^{31}P NMR Hahn-echo spectra were recorded at different magnet fields 4.7 T (batch #3), 11.7 T (batches #1 and #2) or 16.4 T (batch #3) at respective ^{31}P NMR frequencies of 81, 202 and 250 MHz, using the 90-τ-180-τ pulse sequence. Samples were packed into 1.3-mm rotors and spun at a rate of 40 kHz. The interscan delay was 1s and typically 4 K (at 11.7 and 16.4 T) to 48 K (at 4.7 T) scans were accumulated. 2D ^{31}P Exchange Spectroscopy (2D Exsy) was performed using the triple pulse sequence 90 - t_1 - 90 - t_{mix}-90 - t_2 with a mixing time t_{mix} of one rotor period, 25 μs. ^{1}H MAS NMR Hahn-echo spectra were recorded at 11.7 and 16.4 T, ^{19}F MAS NMR at 4.7 T.

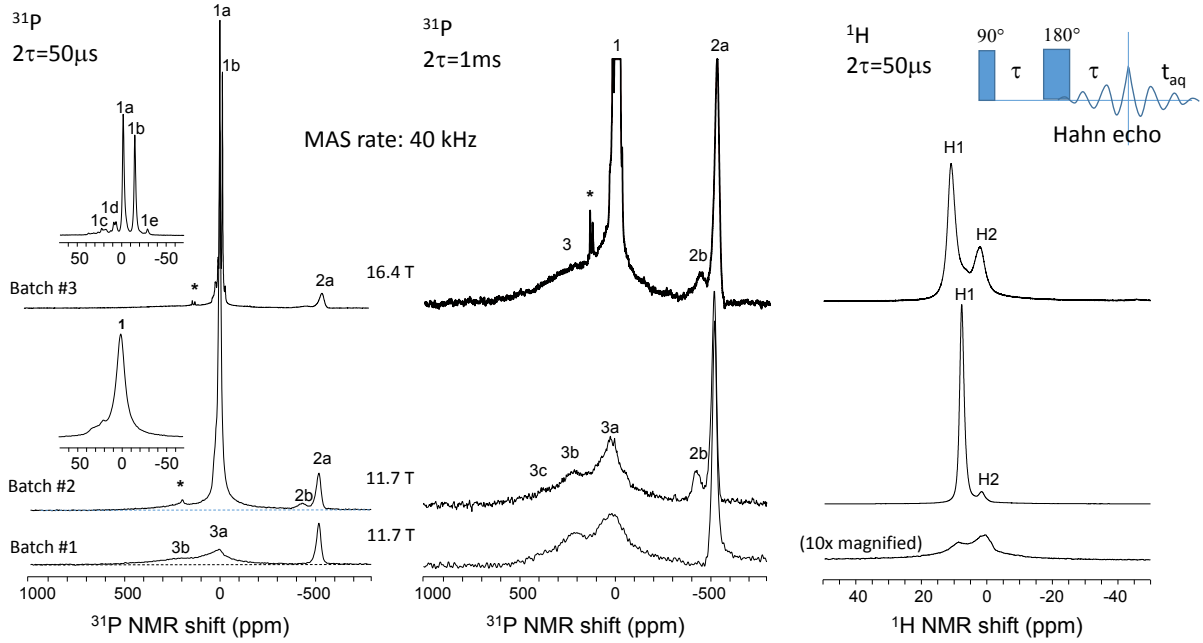

Figure S7. (left, centre) ^{13}P and (right) ^{1}H NMR spectra of three independently synthesized P-DG batches #1, #2 and #3 (bottom, centre, top) recorded at different magnetic fields: (bottom, centre) 11.7 T and (top) 16.4 T. As reflected by the ^{1}H NMR spectra (right), batch #1 was relatively dry, whereas batches #2 and #3 still contained traces of water (peak H1) and acetone (H2) in different ratios. The left and centre columns show Hahn-echo spectra at short and long echo times 2τ of 50 μs and 1 ms, respectively. All batches show a "narrow" ^{31}P signal 2a at -521 ppm (white phosphorus P_4) and broad, overlapping components 3a-c between 0 and 500 ppm (phosphorus embedded in paramagnetic, partly oxidised graphite). The water-containing batches #2 and #3 show an additional "narrow" signal 2b at -445 ppm (variant of P_4 in contact with H_2O), and either a few narrow signals between ±30 ppm (batch #3) or a single signal at 0 ppm (batch #2), which decays fast with echo time and vanishes at 2τ > 1 ms (mobile phosphate oligomers in residual water).

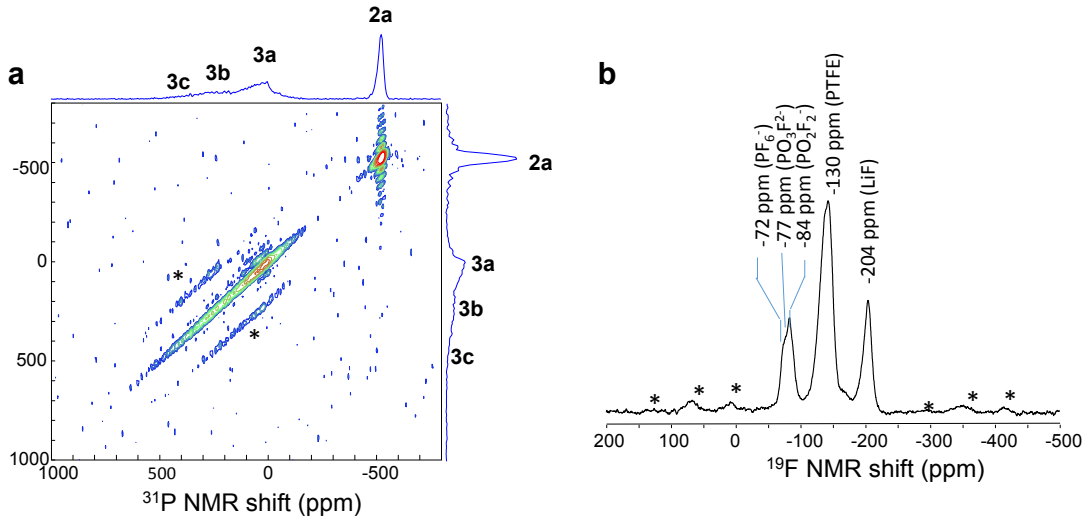

Figure S8. (a) Two-dimensional exchange ^{13}P NMR spectrum of dry P-DG (Batch #1) and (b) ^{19}F NMR spectrum of P-DG (Batch #3) after electrochemically lithiation. The diagonally elongated shape of the overlapping signal components 3a-c in 2D ^{13}P NMR spectrum illustrate the inhomogeneous lineshape. Weak sub-diagonal on both sides of the spectrum diagonal are spinning sidebands. The assignment of the ^{19}F NMR spectrum is indicated above the respective signals. Sample rotation rate: 40 kHz. Spinning sidebands marked with a star

7. Resistivity Measurements

Resistivity measurements were made using a conventional four-point AC transport technique. Contacts were made to the sample with conducting epoxy, cured at 160 C for 2 hours. Current was applied with a custom balanced current source driven by a lock-in amplifier which measured the voltage drop. The response was ohmic for currents $0.001 < I < 1$ mA, and frequency-independent for excitation frequencies $5 < f < 61$ Hz.

Resistivity down to low temperatures was measured in a Quantum Design Physical Properties Measurement System, using both the AC Transport option (a lock-in amplification technique as described above) and the Resistivity option, which applies an alternating DC current. Both techniques gave essentially identical results; the latter was found to be better optimised for high-resistance measurements at low temperature. The typical current applied was 0.04 mA.

Measurements were taken down to 2 K in fields up to 9 T. The resistivity's temperature dependence, ρ(T), was fitted to a modified Arrhenius law $\rho(T) = \rho_0 e^{((\frac{T_0}{T})^{\alpha})}$ where ρ_0, T_0 and α were free parameters. For $T \gtrsim 240$ K, the exponent $\alpha \approx 1$ and the parameter $T_0 \approx 90$ K, indicating Arrhenius behaviour and a band gap $E_g = 2k_bT_0$ of 16 meV (see figure S8). Below 20 K, the exponent $\alpha \approx 0.27$, indicating Mott variable-range hopping in three dimensions (Mott's model predicts $\alpha = 1/4$). This is confirmed by a plot of ln ρ(T) against $T^{-1/4}$ giving a straight line (figure S8). The characteristic hopping temperature is $T_0 \approx 500$ K, corresponding to an activation energy for hopping of around 40 meV.

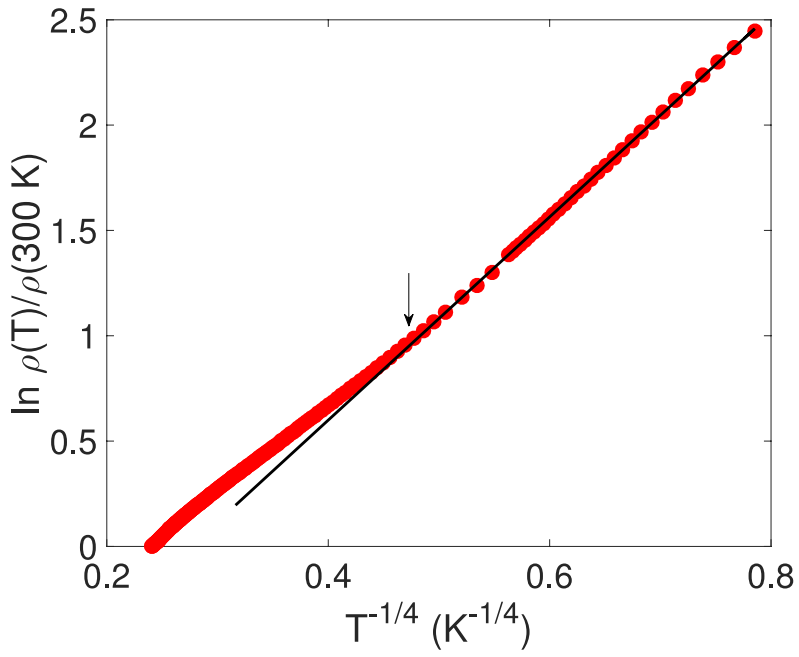

Figure S9. Plot of natural logarithm of the resistivity ratio against $T^{-1/4}$ for the full temperature range. Red markers are data; black line is linear fit, indicating agreement with a three-dimensional variable-range hopping model. Data deviates from the variable-range hopping model above a crossover temperature of approximately 20 K (indicated by the black arrow).

8. Li Binding

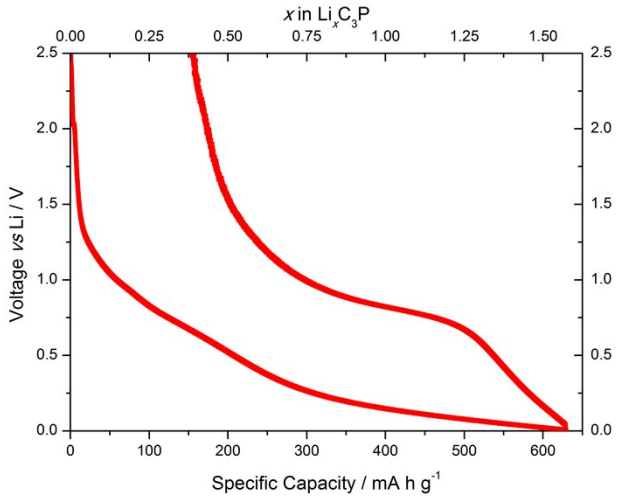

Figure S10. One cycle for the charge and discharge of lithium in P-DG, demonstrating a maximum capacity of 630 mA h g^{-1}.

Figure S9 shows that on 1st discharge (lithium insertion) of P-DG down to 0.005V, a capacity of 630 mA h g^{-1} is achieved. This equates to insertion of just over 1.9 Li per $C_{4.17}P$ unit. Charging to 2.5 V shows the process is not completely reversible, with 470 mA h g^{-1} or 1.42 Li being removed from the material. The loss of capacity is likely due to irreversible electrolyte reaction on the surface of the film, forming a solid electrolyte interface (SEI) layer. Subsequent cycles show a rapidly decreasing capacity due to irreversible Li reaction with either the carbon matrix or embedded P.

References

1. E. P. Kyba, S. T. Liu and R. L. Harris, *Organometallics*, 1983, **2**, 1877–1879.
2. K. Issleib, E. Leissring and H. Meyer, *Tetrahedon Lett.*, 1981, **22**, 4475–4478.
3. T. C. King, P. D. Matthews, H. Glass, J. A. Cormack, J. P. Holgado, M. Leskes, J. M. Griffin, O. A. Scherman, P. D. Barker, C. P. Grey, S. E. Dutton, R. M. Lambert, G. Tustin, A. Alavi and D. S. Wright, *Angew. Chem. Int. Ed. Engl.*, 2015, **54**, 5919–5923.